

# THE PERMANENT MAGNET SYNCHRONOUS MOTOR ROBUST NONLINEAR FEEDBACK CONTROL BASED ON LYAPUNOV METHOD -EXPERIMENTAL EVALUATION-

\*A. FEZZANI    \*S. DRID

\*Laboratory, LSP-IE, University of Batna, Rue Chahid Med El-Hadi Boukhlof BATNA 05000, ALGERIA  
Email: amorfezzani@yahoo.fr

\*ABDESSALAM. MAKOUF

**Abstract:** This paper deals with a robust control intended for permanent magnet synchronous motor. Two approaches are used: the first one a nonlinear input output state feedback linearizing control and second one is a proposed nonlinear feedback control based on Lyapunov method. This second solution shows good robustness with respect to parameter variations, measurement errors and noises. Finally, simulation and experimental results are given to demonstrate the effectiveness and the good performance of the proposed control.

**Key words:** Lyapunov function, permanents magnet synchronous motors, robust nonlinear control.

## 1. Introduction.

The PMSM is becoming more and more popular in servo systems because of its high power density, large torque to inertia ratio and high efficiency [1], [2]. Also the PMSM model is nonlinear coupled and subjected to parameter variation. The PMSM model is described by a fifth-order nonlinear differential equation, where a part of states are not easily measurable, and often perturbed by an unknown load torque. Classical PI controller is a simple method used to control PMSM drives. However the main drawbacks of PI controller are the sensitivity of performances to the system parameter variations and inadequate rejection of external disturbances and load change.

Recently, several nonlinear control methods have been applied to control PMSM considering the nonlinear PMSM dynamics, such as feedback linearization [3], back-stepping [4].

This paper deals with a development of a nonlinear control of current based on Lyapunov Method. Introducing sliding mode control conducts to efficient robustness against parameters variations, measurements errors and noises. The asymptotic stability of the overall system is theoretically proven.

## 2. Model machine

Its dynamic model expressed in the rotor reference frame is given by voltage equations:

$$v_d = R_s I_d + \frac{d\Phi_d}{dt} + p\Omega\Phi_q \quad (1)$$

$$v_q = R_s I_q + \frac{d\Phi_q}{dt} + p\Omega\Phi_d$$

Where the flux expression are given by

$$\Phi_d = L_d I_d + \Phi_f$$

$$\Phi_q = L_q I_q$$

Considering  $I_d$  and  $I_q$  are stats variables (1) can be written as

$$\frac{dI_d}{dt} = -\frac{R_s}{L_d} I_d + \frac{L_q}{L_d} p\Omega + \frac{v_d}{L_d} \quad (2)$$

$$\frac{dI_q}{dt} = -\frac{R_s}{L_q} I_q - \frac{L_d}{L_q} p\Omega I_d - \frac{\Phi_f}{L_q} p\Omega + \frac{v_q}{L_q}$$

The electromagnetic torque is given by

$$T_e = \frac{3}{2} p [(L_d - L_q) I_d I_q + \Phi_f I_q] \quad (3)$$

And the associated equation of motion is

$$J_m \frac{d\Omega}{dt} = T_e - T_L - f_m \Omega \quad (4)$$

Form (2), (3) and (4), the state model is rewritten as:

$$\dot{x} = f_r(x) + g_d(x)v_d + g_q(x)v_q \quad (5)$$

$$y = h(x)$$

Where

$$f_r(x) = \begin{bmatrix} a_{11}x_1 + a_{12}x_1x_2 \\ a_{21}x_2 + a_{22}x_1x_3 + a_{23}x_3 \\ a_{31}x_1x_3 + a_{32}x_2 + a_{33}x_3 + a_{34}T_r \end{bmatrix} = \begin{bmatrix} f_1 \\ f_2 \\ f_3 \end{bmatrix} \quad (6)$$

and

$$g_d(x) = \begin{pmatrix} \lambda_d \\ 0 \\ 0 \end{pmatrix}, \quad g_q(x) = \begin{pmatrix} 0 \\ \lambda_q \\ 0 \end{pmatrix}$$

$$v_s = [v_d \quad v_q]^T, \quad [x_1 \quad x_2 \quad x_3] = [I_d \quad I_q \quad \Omega]^T$$

$$a_{11} = -\frac{R_s}{L_d}, \quad a_{12} = \frac{L_q}{L_d} p, \quad a_{21} = -\frac{R_s}{L_q}, \quad a_{22} = -\frac{L_d}{L_q} p,$$

$$a_{23} = -\frac{\Phi_f}{L_q} p, \quad a_{31} = \frac{3p}{2J} (L_d - L_q), \quad a_{32} = \frac{3p}{2J} \Phi_f,$$

$$a_{33} = -\frac{f}{J}, \quad a_{34} = -\frac{1}{J}, \quad \lambda_d = 1/L_d, \quad \lambda_q = 1/L_q$$

### 3. Input output feedback linearization control.

The outputs to be controlled are the motor speed  $\Omega$  and the stator current  $I_d$ , i.e. the function  $h(x)$  in (5) is defined as

$$h(x) = \begin{bmatrix} I_d \\ \Omega \end{bmatrix} \quad (7)$$

The derivative of (7) is given by

$$\begin{bmatrix} \dot{y}_1 \\ \dot{y}_2 \end{bmatrix} = \begin{bmatrix} L_f h_1(x) \\ L_f^2 h_2(x) \end{bmatrix} + D(x) \begin{bmatrix} v_d \\ v_q \end{bmatrix} \quad (8)$$

The systems has relative degree 1 for  $I_d$  and 2 for  $\Omega$ ,  $D(x)$  is the decoupling matrix defined by

$$D(x) = \begin{bmatrix} \lambda_d & 0 \\ \lambda_d a_{31} x_2 & \lambda_q (a_{32} + a_{31} x_1) \end{bmatrix} \quad (9)$$

and

$$L_f h_1(x) = a_{11} x_1 + a_{12} x_2 x_3 \quad (10)$$

$$L_f^2 h_2(x) = a_{31} x_2 f_1(x) + (a_{32} + a_{31} x_1) f_2(x) + a_{33} f_3(x) + a_{34} \dot{T}_L + a_{33} a_{34} T_L \quad (11)$$

Since  $|D(x)| = \lambda_d \lambda_q (a_{32} + a_{31} x_1) \neq 0$ , then  $D(x)$  is not singular (machine with permanent magnets) and the MIMO system is input-output linearizable since the state feedback control given by reduces Input-Output map to:

$$\begin{bmatrix} v_d \\ v_q \end{bmatrix} = D^{-1}(x) \begin{bmatrix} -L_f h_1(x) \\ -L_f^2 h_2(x) \end{bmatrix} + \begin{bmatrix} v_1 \\ v_2 \end{bmatrix} \quad (12)$$

Where  $v = [v_1 \quad v_2]^T$  is the new input vector.

$$\begin{bmatrix} \dot{y}_1 \\ \dot{y}_2 \end{bmatrix} = \begin{bmatrix} v_1 \\ v_2 \end{bmatrix} = \begin{bmatrix} k_{11}(I_d - I_{d\_ref}) \\ k_{21}(\Omega - \Omega_{ref}) + k_{22}(\dot{\Omega} - \dot{\Omega}_{ref}) \end{bmatrix} \quad (13)$$

A bloc diagram of control nonlinear input-output is shown in fig.1

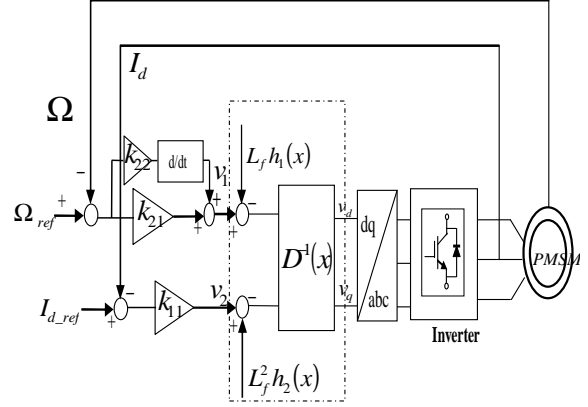


Fig. 1. Bloc diagram of PMSM control (FLIOC) scheme

The drawback of (12) is that it requires exact knowledge of the motor parameters and any variation in the parameters or the load torque will deteriorate the controller performances. In order to overcome this problem feedback nonlinear control based on Lyapunov theory is proposed.

### 4. Robust nonlinear feedback control based on Lyapunov method

The suggested PMSM control scheme is shown in Fig. 2. We can see that only one PI speed controller is used and the currents are feedback-controlled in association with a sliding mode controller. We can also note the placement of the estimator block which evaluates the feedback function  $f_1$  and  $f_2$  given by (6).

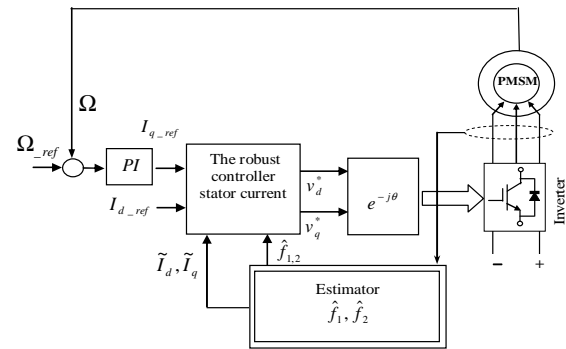


Fig. 2. Bloc diagram of nonlinear feedback control based on Lyapunov method system.

To determine the control feedback, starting with the equation (2) represented as follow

$$\begin{aligned}\frac{dI_d}{dt} &= \lambda_d v_d + f_1 \\ \frac{dI_q}{dt} &= \lambda_q v_q + f_2\end{aligned}\quad (14)$$

Where

$$\begin{aligned}f_1 &= a_{11}x_1 + a_{12}x_1x_2 \\ f_2 &= a_{21}x_2 + a_{22}x_1x_2 + a_{23}x_3\end{aligned}$$

To prove the stability of system considering the candidate Lyapunov function [2]:

$$V = 0.5(I_d - I_{d\_ref})^2 + 0.5(I_q - I_{q\_ref})^2 \quad (15)$$

The time derivative is given by

$$\dot{V} = (I_d - I_{d\_ref})(\dot{I}_d - \dot{I}_{d\_ref}) + (I_q - I_{q\_ref})(\dot{I}_q - \dot{I}_{q\_ref}) \quad (16)$$

Taking in to account of (14) in (16) yields we obtain

$$\begin{aligned}\dot{V} &= (I_d - I_{d\_ref})(\lambda_d v_d + f_1 - \dot{I}_{d\_ref}) \\ &\quad + (I_q - I_{q\_ref})(\lambda_q v_q + f_2 - \dot{I}_{q\_ref})\end{aligned}\quad (17)$$

Selecting the control law as

$$\begin{aligned}v_d &= \frac{1}{\lambda_d}(-f_1 + \dot{I}_{d\_ref} - K_1(I_d - I_{d\_ref})) \\ v_q &= \frac{1}{\lambda_q}(-f_2 + \dot{I}_{q\_ref} - K_2(I_q - I_{q\_ref}))\end{aligned}\quad (18)$$

Where  $K_1$ ,  $K_2$  are positive gains and inserting them (17), we found:

$$\dot{V} = -K_1(I_d - I_{d\_ref})^2 - K_2(I_q - I_{q\_ref})^2 < 0 \quad (19)$$

If  $K_1$ ,  $K_2$  are chosen, the time negativity of derivative of Lyapunov function  $\dot{V}$  is satisfied, and control system will be stabilized.

We concluded that

$$\begin{aligned}\lim_{t \rightarrow \infty} (I_d - I_{d\_ref}) &= 0 \\ \lim_{t \rightarrow \infty} (I_q - I_{q\_ref}) &= 0\end{aligned}\quad (20)$$

#### 4.1 Robust Feedback nonlinear control

The nonlinear functions  $f_i$  involved in the state-space model (14) are strongly affected by the conventional effects of PMS motors, such temperature, saturation, skin effects and the noise measurements. Since the control law developed in the preceding section is based

on exact knowledge of these functions  $f_i$ , one can expect that in a real situation. Our objective is to determine a new control law robust to parameter variations and measurement noise. Globally, we can write

$$f_i = \hat{f}_i + \Delta f_i \quad (21)$$

where  $\hat{f}_i$  is the true nonlinear feedback function (NLFF),  $f_i$  is the effective NLFF and  $\Delta f_i$  is the NLFF variation around  $f_i$ . The  $\Delta f_i$  can be generated from all of the parameters and variables as indicated above. We assume that all of the  $\Delta f_i$  are bounded as follows:  $|\Delta f_i| < \beta_i$  where the  $\beta_i$  are known bounds. Knowledge of the  $\beta_i$  is not difficulties obtain, since one can use a sufficiently large number to satisfy the constraint  $|\Delta f_i| < \beta_i$ .

The  $\Delta f_i$  can be generated from the all of the parameters and variations as indicated above.

Substitution of (21) into (14) yields:

$$\begin{aligned}\frac{dI_d}{dt} &= \lambda_d v_d + \hat{f}_1 + \Delta f_1 \\ \frac{dI_q}{dt} &= \lambda_q v_q + \hat{f}_2 + \Delta f_2\end{aligned}\quad (22)$$

Select the control law as

$$\begin{aligned}v_d &= \frac{1}{\lambda_d}(-\hat{f}_1 + \dot{I}_{d\_ref} - K_1(I_d - I_{d\_ref}) - K_{11} \text{sign}(I_d - I_{d\_ref})) \\ v_q &= \frac{1}{\lambda_q}(-\hat{f}_2 + \dot{I}_{q\_ref} - K_2(I_q - I_{q\_ref}) - K_{22} \text{sign}(I_q - I_{q\_ref}))\end{aligned}\quad (23)$$

Where  $K_{ii} \geq \beta_i$ ,  $K_i > 0$  and  $i = 1, 2$ .

The Lyapunov function relativity to (22) is defined by

$$V = 0.5(I_d - I_{d\_ref})^2 + 0.5(I_q - I_{q\_ref})^2 \quad (24)$$

We have

$$\begin{aligned}\dot{V} &= (I_d - I_{d\_ref})(\Delta f_1 - K_{11} \text{sign}(I_d - I_{d\_ref})) \\ &\quad + (I_q - I_{q\_ref})(\Delta f_2 - K_{22} \text{sign}(I_q - I_{q\_ref})) + \dot{V} < 0\end{aligned}\quad (25)$$

Where  $\dot{V}$  is given by (17). Hence the  $\Delta f_i$  variations can be absorbed if we take

$$K_{111} > |\Delta f_1| \quad (26)$$

$$K_{22} > |\Delta f_2|$$

These inequalities are satisfied since  $K_i > 0$  and

$$|\Delta f_i| < \beta_i < K_{ii}. \text{ Finally, we can write}$$

$$\dot{V}_1 < \dot{V} < 0 \quad (27)$$

Insuring the negativity of Lyapunov function. Hence, using Lyapunov theorem [2], we conclude that

$$\lim_{t \rightarrow \infty} (I_d - I_{d\_ref}) = 0 \quad (28)$$

$$\lim_{t \rightarrow \infty} (I_q - I_{q\_ref}) = 0$$

The design of these robust controllers, resulting from (27), is given in Fig.3.

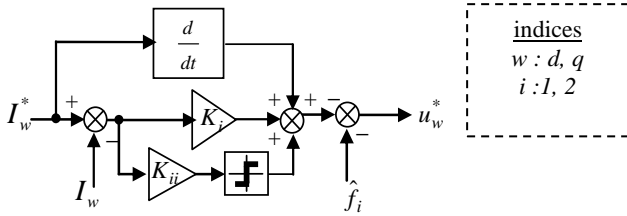


Fig. 3. Design of a robust controller.

## 5. Simulation results

Two schemes have been implemented: 1) a feedback linearizing input output Control (FLIOC) and 2) the proposed nonlinear feedback control based on Lyapunov Method scheme (NLFC). To the end of more significant comparison between the two schemes, the tests have been conducted to analyze and compare the performance of the PMSM in terms of accuracy, dynamic performance and load disturbance rejection. The parameters of the PMSM used in the simulation are given as: rated voltage  $V=511$  V, number of poles  $p=3$ , armature resistance  $R_s=1.4\Omega$ , Stator inductances  $L_d=0.0066$  H,  $L_q=0.0058$  H, viscous damping  $f_m=0.00038$  N.m.s/rad, moment of inertia  $J_m=0.0016$  kg.m<sup>2</sup>, rotor flux  $\Phi_f=0.1546$  wb, rated torque  $T_n=10$  N.m.

Figs. 4 and 5 shows the PMSM response to square-wave speed reference 200 rad/s, using the FLIOC and NLFC. The NLFC PMSM drive speed trajectory is characterized by zero steady-state error and very fast dynamic response. The comparison between the FLIOC and NLFC speed transients, reported in Figs. 6 and 7, highlights the better performance of the proposed control. The considerations indicated above are confirmed by the following test imposing a 5-Hz sinusoidal reference speed of 10rad/s peak value. The comparison between the actual speed profiles, Fig. 8 shows a better dynamic response of FLL scheme.

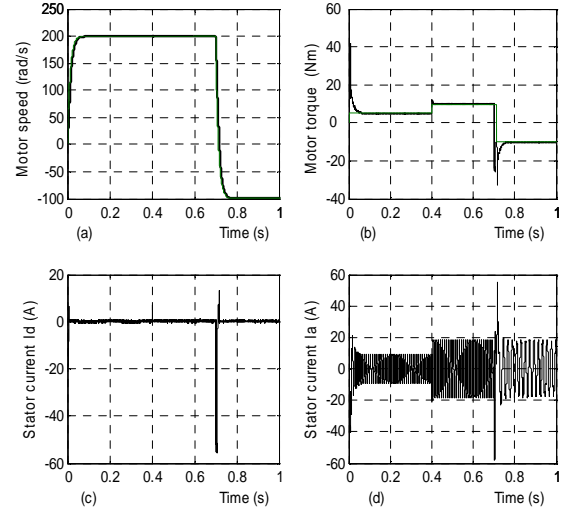


Fig.4. Simulation results of feedback linearizing control : a) motor speed b) motor torque c) stator current Id d) stator current Ia (A)

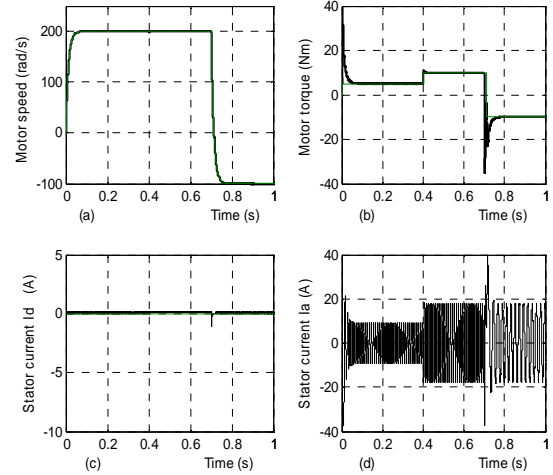


Fig.5. Simulation results of Nonlinear feedback Control Based on Lyapunov Method : a) motor speed b) motor torque c) stator current Id d) stator current Ia (A)

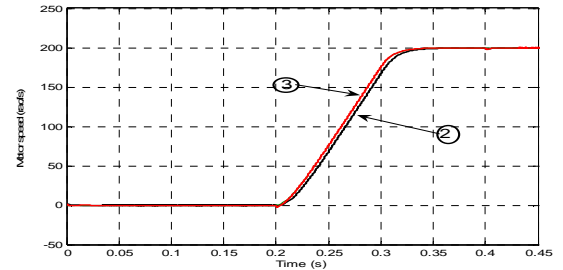


Fig. 6. Comparison between FLIOC (tr.2) and NLFC (tr.3) speed transient evolutions

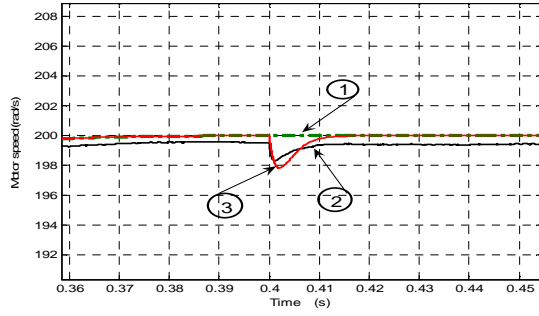


Fig. 7. Zoom of FLIOC (tr.2) and NLFC (tr.3) speed transient. (tr.1 reference speed).

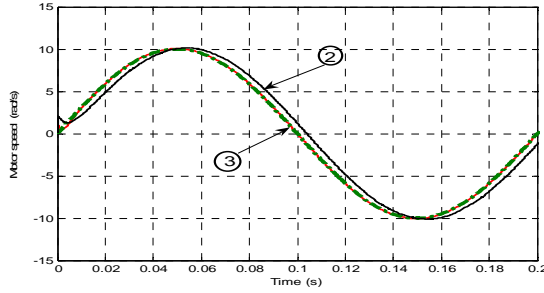


Fig. 8. Comparison between FLIOC (tr.2) and NLFC (tr.3) speed evolutions to the application of the same sinusoidal reference speed. (Crest value 10 rad/s, frequency 5Hz)

To test robustness of feedback control. The simulation involves the following operating sequences:  
The PMSM started with a constant acceleration after 0.1s, the speed was maintained to 10 rad/s, while the motor is loaded with a constant torque of 5 Nm at starting. Then the motor is loaded with a constant torque of 10 Nm at  $t=0.4s$ . at  $t=0.7s$ , the speed change from 10 rad/s to 0 rad/s with same constant load torque. Maintaining a reference current  $I_d$  to zero. Two sets of simulation tests are carried out.

The first set is carried out with stator resistance having a mismatch of 100% at  $t=0.5s$  using the control law given by (12) the results of this test set are shown in Fig. 9 (tr.2). It is clear that when considering stator resistance uncertainty, a very large steady state error occurred in motor speed.

Finally the motor having a  $f_i$  (NLFF) mismatch of 300% at  $t=0.5s$  and in the presence of noise is simulated using the proposed control (23). The results are shown in Fig. 9 (tr.3). The control shows better speed response even in the presence of parameter uncertainty and measurement noises.

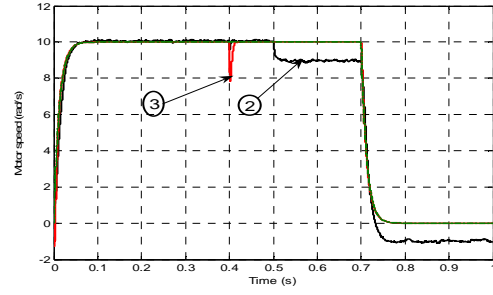


Fig. 9. Comparison between FLIOC (tr.2) and NLFC (tr.3) speed transient evolutions with parameter uncertainty and measurement noises.

## 6. Experimental the al system

The basic structure of the laboratory setup is depicted in Fig. 10. The DC motor is used as a load. The PMSM stator is fed by a converter controlled directly by the DS1103 board. The dSPACE DS1103 PPC is plugged in the host PC. The encoder is used for the measure mechanical speed. The sensors used for the currents and voltages measure are respectively LA-25NP and LV-25P. The Interface to provide galvanic isolation to all signals connected to the DS1103 PPC controller.

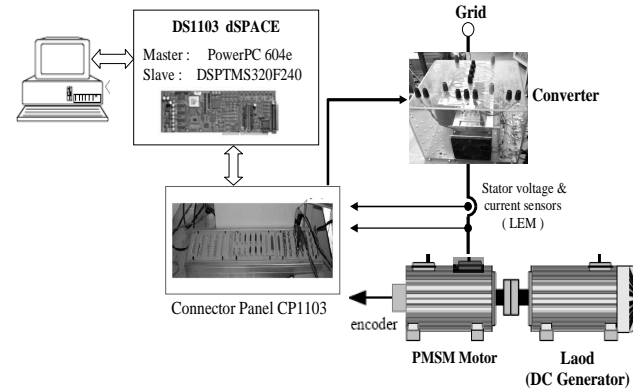


Fig.10 Structure of the laboratory setup

### 6.1 Reference profiles and machine parameters

To test the speed tracking, we applied two kinds of speed references. In the first, the PMSM is started with a constant acceleration  $33.33 \text{ (rd/s}^2\text{)}$ , after 3 s, the speed was maintained to  $100 \text{ (rd/s)}$ . After that, a reversal speed test was applied to the loaded machine at 21 s, where the speed changed to  $-100 \text{ (rd/s)}$ , Fig. 11. The load is 1 mN. In the second, a sinusoidal speed reference of magnitude 100 rad/s with frequency 0.05 Hz. The machine was loaded at 1 mN. (see Figs. 11a and 11b).

The machine parameters are given as follows:

$R_s=11\Omega$ ;  $L_d=0.995 \text{ H}$ ;  $L_q=0.885\text{H}$ ;  $p=2$ ;  $J=0.025\text{SI}$ ;  $f=0.0001\text{SI}$ ;  $\Phi_f=0.15\text{wb}$

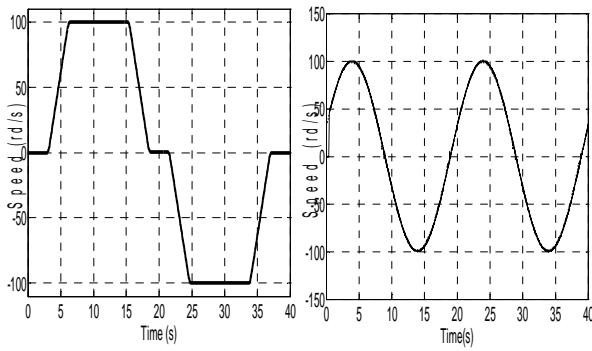


Fig. 11 Speed references versus time

## 6.2 Experimental results

Fig. 12 and 14 present the speed response versus time according to the profiles described above.

The actual speed converges to the reference speed very quickly with zero steady-state error and almost without any overshoot/undershoot in real-time.

Figs. 13 and 15 show, respectively, the stator phase current and the quadratic current  $I_q$  versus time during the test.

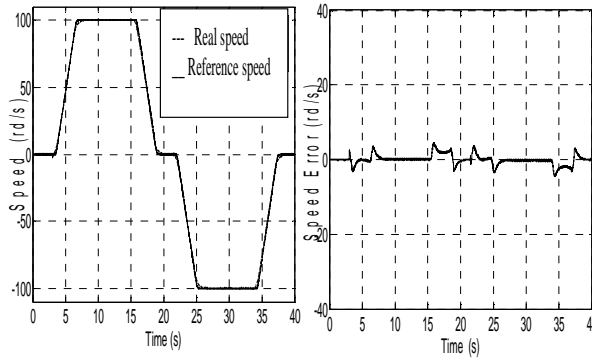


Fig. 12 Speed response versus time and speed error versus time

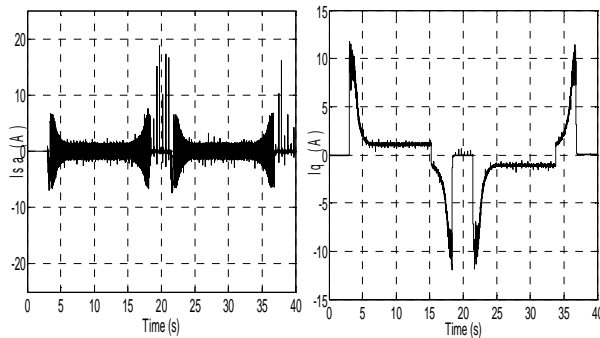


Fig. 13 Stator phase current versus time and  $I_q$  current versus time

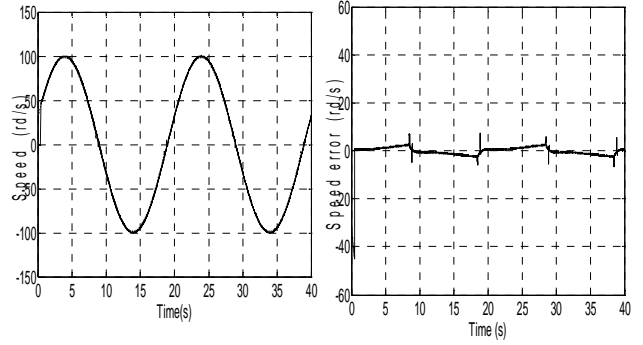


Fig. 14 Speed response versus time and speed error versus time

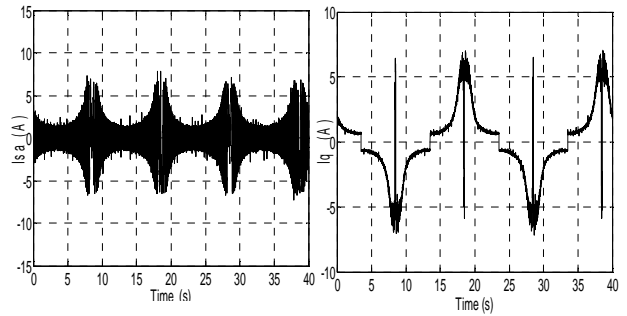


Fig. 15 Stator phase current versus time and  $I_q$  current versus time

Figs. 10 and 12 show speed and stator current response versus time; we observe that with the proposed control a good tracking speed and currents were achieved.

## 7. Conclusion

This paper presents two control schemes for the PMS motor. Firstly, an input-output linearizing control is developed. Secondly, a feedback nonlinear control based on the Lyapunov method is proposed in order to reduce the effects of parametric variations and measurement noise.

The theoretical study of the proposed control technique (NLFC) has been discussed, and the simulation results of the overall system have been presented to prove the effectiveness of this control strategy. Control robustness is achieved by a sliding-mode controller in order to reduce the effects of parametric variations, uncertainties, and measurement noise.

The control stability is verified via Lyapunov stability analysis. From the simulation and experimental results for the proposed scheme, very well performances for both high and low speed are achieved. The proposed control is robust to parameter changes.

## References

1. M. Bodson, J. Chiasson, and R. Novotnak: *High performance induction motor control via input output linearization*. IEEE. Cont. Syst Mag., Vol, 14, pp. 25–33, 1994.
2. H. Khalil: *Nonlinear systems*. Prentice–Hall, 2ed edition, Printed in USA, 1996.
3. B. Gracar, P. Cafuta and M. Znidaric: *Nonlinear control of synchronous servo drive*. in IEE Conf. Control, Coventry, U.K, pp. 1198–1203, March. 1994.
4. J.J. Carroll, D.M. Dawson: *Tracking control of permanent magnet brushless dc motors using partial state feedback* in 2nd IEEE conf. Contr, application .pp. 147–152, Sep. 1993.
5. W. Leonhard: *Control of electrical drives*. Epringer, Bertin, Germany, 1996.
6. R. Marino, P. Tomei: *Nonlinear control desing*. Englewood Cliffs, NJ: Prentice Hall 1995.
7. T.K. Boukas and T.G, Habetler: *High performance induction motor speed control using exact feedback linearization with state and state derivative feedback*. IEEE Trans. On Power Electronics Vol, 19, no. 4, pp. 1022–1028, 2004.
8. Thomas Von Raumer, Jean Michel Dion and Luc Dugard: *Combined nonlinear controller and full order observer design for induction motor*. IEEE, IECON'94 Conference Bologna 5–9, September 1994.
9. G. Sturtzer, E. Smigiel: *Modélisation et commande des moteurs triphasés*. Edition Ellipes. 2000.
10. M. Bodson, and J. Chiasson: *Differential-Geometric Methods*. International Journal Robust and Nonlinear Control, pp. 923–954, 1998.
11. A. Kaddouri : *Etude d'une commande non linéaire adaptative d'une machine synchrone à aimants permanents*. Thèse de doctoral, Université LAVAL, QUEBEC, 2000.
12. P. Pillay and Krishnan: *Modeling, simulation and analysis of permanent magnet motor drives*, part I: the permanent magnet motor drive," IEEE Trans. On Industry applications, Vol, 25, no. 2, pp. 265–273, March. /April. 1989.
13. A. H. yousef and A. M. wahba: *Adaptive fuzzy mimo control of induction motor*. Expert systems with applications, Vol, 39, pp. 4171–4175, 2008.
14. S. Drid, M. Tadjine and M.S. Naït-Saïd: *Robust Backstepping Vector control for the Doubly Fed Induction Motor*. IET Control Theory Appl., Vol. 1, no. 4, July. 2007.
15. S. Drid, A. Makouf, M.S. Naït-Saïd and M. Tadjine, "Highly Efficient Control of the Doubly Fed Induction Motor," Journal of Electrical Engineering & Technology Vol.2, no.43, pp. 478~484, December 2007.
16. S. Drid, A. Makouf, M.S. Naït-Saïd and M. Tadjine: *The Doubly Fed Induction Generator Robust Vector Control based on Lyapunov Method*. Transactions on Systems, Signals and Devices, Vol. 4, no. 2, pp. 237-

250 (Issues on Power Electrical Systems) published by Shaker-Verlag (Germany), 2009.